On Pacific Subtropical Cell Variability over the Second Half of the Twentieth Century

RICCARDO FARNETI

Earth System Physics Section, Abdus Salam International Centre for Theoretical Physics, Trieste, Italy

SUNEET DWIVEDI

Department of Atmospheric and Ocean Sciences, University of Allahabad, Allahabad, India

FRED KUCHARSKI

Earth System Physics Section, Abdus Salam International Centre for Theoretical Physics, Trieste, Italy, and Center of Excellence for Climate Change Research/Department of Meteorology, King Abdulaziz University, Jeddah, Saudi Arabia

FRANCO MOLTENI

European Centre for Medium-Range Weather Forecasts, Reading, United Kingdom

STEPHEN M. GRIFFIES

NOAA/Geophysical Fluid Dynamics Laboratory, Princeton, New Jersey

(Manuscript received 22 November 2013, in final form 17 June 2014)

ABSTRACT

The evolution of the Pacific subtropical cells (STC) is presented for the period 1948–2007. Using ocean models of different resolutions forced with interannually varying atmospheric forcing datasets, the mechanisms responsible for the observed STC weakening and late recovery during the period of study are analyzed. As a result of the STC weakening (strengthening), warming (cooling) trends are found in the equatorial Pacific sea surface temperatures (SSTs). Model results agree well with observed estimates of STC transport, STC convergence, and equatorial SST anomalies. It is shown that subtropical atmospheric variability is the primary driver of the STC and equatorial SST low-frequency evolution and is responsible for both the slowdown during the second half of the twentieth century and the rebound at the end of the century. Subtropically forced STC variability is identified as a major player in the generation of equatorial Pacific decadal SST anomalies, pacing tropical Pacific natural climate variability on interdecadal time scales, as observed in historical records. The natural mode of variability has implications for the evolution of equatorial SST in the coming decades under the concomitant effects of climate change.

1. Introduction

The Pacific meridional overturning circulation (PMOC) is understood in terms of the subtropical cells (STCs), shallow meridional overturning cells connecting tropical upwelling zones with subtropical subduction zones in both hemispheres (Liu 1994; McCreary and Lu 1994; Schott et al. 2004). The Pacific STCs have been suggested to serve as a pathway for tropical–extratropical atmosphere–ocean interactions (Kleeman et al. 1999; Nonaka et al. 2002; Solomon et al. 2003; Solomon 2010; Farneti et al. 2013). Theories for the STC relate their strength to the wind stress at the subduction cutoff latitude θ ($\theta \sim 15°$) that dynamically defines the boundary between tropical and subtropical gyres (McCreary and Lu 1994; Lu et al. 1998; McPhaden and Zhang 2002, hereafter MZ02). Through the STCs, the water flows out of the tropics within the surface layer, subducts in the subtropics, flows equatorward within the thermocline, and upwells in the eastern equatorial ocean (McCreary and Lu 1994; Johnson and McPhaden 1999; Solomon and Zhang 2006). The STCs are important for setting up the thermocline mean structure in the tropics by subducting water in the subtropics and

Corresponding author address: Riccardo Farneti, Earth System Physics Section, Abdus Salam International Centre for Theoretical Physics, Strada Costiera 11, Trieste, Italy.
E-mail: rfarneti@ictp.it

DOI: 10.1175/JCLI-D-13-00707.1

ventilating the equatorial ocean (Cheng et al. 2007). Low-frequency modulations of the equatorial Pacific have consequences on the properties of El Niño events that are nontrivial and difficult to predict in terms of both activity and frequency (Collins et al. 2010; Fedorov and Philander 2001). Moreover, a dynamically changing Pacific Ocean circulation has significant implications for equatorial upwelling, which affects not only tropical Pacific sea surface temperatures (SSTs), but also the exchange of CO_2 across the air–sea interface and the supply of nutrients to the biologically productive surface layer of the ocean (MZ02).

MZ02, using observational data for the period 1950–99, have found that the meridional overturning circulation in the upper Pacific Ocean has been slowing down during this period. McPhaden and Zhang (2004, hereafter MZ04) have later noted a rebound in the circulation since 1998, suggesting significant decadal variability in the STCs. However, there is still a debate on whether the STC varies on decadal time scales (Cheng et al. 2007) or not (Schott et al. 2007), whether coupled models can reproduce such variability (Zhang and McPhaden 2006, hereafter ZM06), and what the implications could be for tropical Pacific climate variability.

The Pacific basin is characterized by modes of natural low-frequency variability, such as the interdecadal Pacific oscillation (IPO), of which the Pacific decadal oscillation (PDO) is the Northern Hemisphere manifestation (Mantua et al. 1997); both of these oscillations are at least partially equatorially forced and are able to imprint significant anomalies on the ocean. However, the Pacific Ocean is also affected by anthropogenic warming, so a proper identification of external forcing and internally generated variability is desirable (Meehl et al. 2013). Recently, much effort has been devoted to the identification of the causes of the slowdown in the rate of surface warming (the so-called warming hiatus), attributing to the equatorial Pacific SST a primary role in explaining the missing heat (Kosaka and Xie 2013; England et al. 2014). Present-generation uninitialized climate models are not able to properly represent the observed wind trends—and hence the SST—in the Pacific, resulting in an overestimation of global warming over the past decades (Fyfe et al. 2013). Understanding the low-frequency natural variability of the equatorial Pacific might therefore provide some insight into its future evolution under ongoing increases of atmospheric greenhouse gases.

Recently, Farneti et al. (2013), building on previous studies (Kleeman et al. 1999; Nonaka et al. 2002; Klinger et al. 2002; Solomon et al. 2003), have proposed an atmosphere–ocean mechanism involving interactions between the tropics and the northern subtropics for the generation of low-frequency tropical Pacific SST variability. The modeling study of Farneti et al. (2013) used an ocean general circulation model (OGCM) forced with flux anomalies (mostly wind) obtained through the integration of an atmospheric model forced with observed Pacific SST decadal anomalies. Farneti et al. (2013) also developed an analytical framework in order to explore the minimal model and the parameter space for the generation of the tropical variability.

Here, by analyzing OGCMs forced with interannually varying atmospheric forcing datasets between 1948 and 2007, we discuss the evolution of the STC over the past 60 years and identify the drivers of its variability, as well as its relationship with the observed and modeled equatorial SST anomalies. In particular, we confirm the primary role of subtropical winds in driving the STC and associated equatorial SST variability. We also expand on the results of Farneti et al. (2013) by showing the quasi-equatorially symmetric nature of the mechanism, whereby the Southern Hemisphere is actually producing the largest equatorward transport anomaly, as revealed by observations. Finally, and contrary to coupled models (Solomon and Zhang 2006; ZM06), we show the ability of OGCMs forced with atmospheric reanalysis datasets to reproduce both the STC transport anomalies and the equatorial SST variability during the past 60 years. The tropical–subtropical ocean–atmosphere interaction provides an explanation for a large fraction of the observed equatorial Pacific SST variability during the twentieth century. As a natural mode of variability, the mechanism also provides a sense for the future evolution of equatorial SST under the concomitant effects of climate change.

2. The models and experiments

We use the National Oceanic and Atmospheric Administration/Geophysical Fluid Dynamics Laboratory (NOAA/GFDL) Modular Ocean Model (MOM) (Griffies et al. 2005). MOM is run globally at three different horizontal and vertical resolutions. The fine-resolution version, MOM-p25, is the ocean–ice component from the GFDL Climate Model version 2.5 (CM2.5) that is documented in Delworth et al. (2012). The oceanic resolution is ¼° (or ~28 km) at the equator and progressively refines toward the poles, with 50 levels in the vertical. Because of the finer resolution, MOM-p25 does not use a parameterization of mesoscale eddy mixing but only a parameterization for the effects of submesoscale, mixed layer eddies (Fox-Kemper et al. 2011). The second version, MOM-1, is configured at 1° resolution in the horizontal, with a refinement to ⅓° near the equator and 50 vertical levels. The coarse-resolution version, MOM-2, is run at 2° resolution in the horizontal, with a refinement to 1° near the equator and 30 vertical levels. In MOM-1 and MOM-2, mesoscale eddy-induced transports are parameterized

using the approach of Ferrari et al. (2010), with a value of 600 (800) $m^2 s^{-1}$ for the neutral diffusivity in MOM-1 (MOM-2). Further details on physical parameterizations of the ocean are provided in Griffies et al. (2005), Dunne et al. (2012), and Delworth et al. (2012).

The models are forced with the Coordinated Ocean–Ice Reference Experiments version 2 (CORE-II) interannually varying air–sea forcing datasets (Griffies et al. 2009; Large and Yeager 2009) from the years 1948 to 2007, and they are run for five repeating cycles of the 60-yr forcing. Only the last cycle is analyzed as a hindcast simulation, with the previous four cycles regarded as a spin-up period (Danabasoglu et al. 2014). We use interannually varying CORE-II precipitation, radiation, sea level pressure, specific humidity at 10 m, air temperature at 10 m, and zonal and meridional wind at 10 m to force the ocean model. To reduce drift, weak restoring is applied to the surface salinity of the top layer (of 10 m thickness) by relaxing to the *World Ocean Atlas 2009* (*WOA09*; http://www.nodc.noaa.gov/OC5/WOA09/netcdf_data.html) with a time scale of 60 days in MOM-p25 and MOM-1 and 55 days in MOM-2. No sea surface temperature restoring is applied anywhere. Models are characterized by different biases of different magnitude, but trends will be shown to be consistent throughout the different resolutions.

3. Results

We start by analyzing the PMOC during the 60-yr period in the models. The linear trend map of the PMOC is shown in Fig. 1 for the upper 225 m for all models. A decreasing trend (significant at the 95% level) extending to $\sim \pm 15°$ and of about 0.25 Sv yr^{-1} (1 Sv = 10^6 $m^3 s^{-1}$) is clearly evident during 1948–2007. It may also be noticed from Fig. 1 that subsurface trend values are higher compared to surface values, with the highest values simulated between 50- and 200-m depth. The highest PMOC trend values in the subsurface layer suggest the importance of subtropical subduction and equatorward transport anomalies, rather than a shallow equatorial mechanism involving, for example, tropical cells only. Indeed, the negative trends extend far beyond the latitudes and depths that characterize the shallow tropical cells, which are confined to a few degrees around the equator and the upper 50 m (Lu et al. 1998). The PMOC climatology, defined by the time-mean meridional streamfunction computed over the Pacific basin, is superimposed as contours in Fig. 1.

As in MZ02, we compute the interior pycnocline transport, defined as the equatorward transport at both 9°N and 9°S zonally averaged from the eastern boundary to 145°E in the NH and 160°E in the SH. Pycnocline transport is achieved by integrating the flow within potential density classes from 22 to 26 σ_θ ($\sigma_\theta = \rho_\theta - 1000$, where ρ_θ is in kg m^{-3}).

Figure 2a shows the modeled equatorward pycnocline transport at 9°N and 9°S. The models agree well with observations from MZ04 both in terms of magnitude and variability. The weakening in the last decades of the twentieth century (though interrupted by interannual fluctuations) and the rebound at the end of the century are well captured. The equatorial transport convergence is shown in Fig. 2b together with the historical reconstruction from ZM06, again showing good agreement with observations. We note that the rebound straddling the year 2000 seems underestimated by the models. Given that the modeled transports approach the observational data as the resolution refines, we argue that differences might be due to the resolution and physics in the models. Hence, although transports get weaker as the resolution is reduced, the long-term trends are well captured by all models.

The tropical Pacific SST, consistent with the observed data, has undergone a substantial warming of about 0.03°C yr^{-1} during the 1948–2007 period (not shown). An analysis of the SST time series reveals that equatorial SSTs were indeed anomalously warm until the late 1990s (Fig. 3a), overall showing an IPO/PDO-like pattern, consistent with a reduction in the advection of cold subtropical pycnocline water from the late 1950s to the 1990s. However, the anomalies reversed sign straddling the year 2000 (Fig. 3b), as was also shown by Cheng et al. (2007), consistent with the strengthening of the STC and the associated meridional export of heat out of the equatorial region into the subtropics. SST anomalies shown in Fig. 3a are for the fine-resolution model MOM-p25, but they are consistent in pattern and magnitude for all models. To better quantify the link between STC variations and equatorial Pacific SST, we compute the correlation between the NIÑO-3.4 index and STC convergence. The correlation between these two indices is −0.74, −0.75, and −0.82 for MOM-p25, MOM-1, and MOM-2, respectively. Thus, although causality cannot be inferred from these correlations, a large fraction of the equatorial Pacific SST low-frequency anomalies is tied to the variability in wind-driven STCs and associated upwelling anomalies, as previously suggested in MZ02 and Cheng et al. (2007).

Anomalies from the Hadley Centre Sea Ice and Sea Surface Temperature (HadISST) dataset (Rayner et al. 2003) dating back to 1900 for the equatorial Pacific Ocean (9°S–9°N and 180°–90°W) are shown in Fig. 4 together with the MOM-p25 SSTs for the period covered. Equatorward convergence anomalies, smoothed with a 10-yr running mean, for MOM-p25 and the observed estimates from ZM06 are also plotted in Fig. 4. The model is capturing the initial negative anomalies,

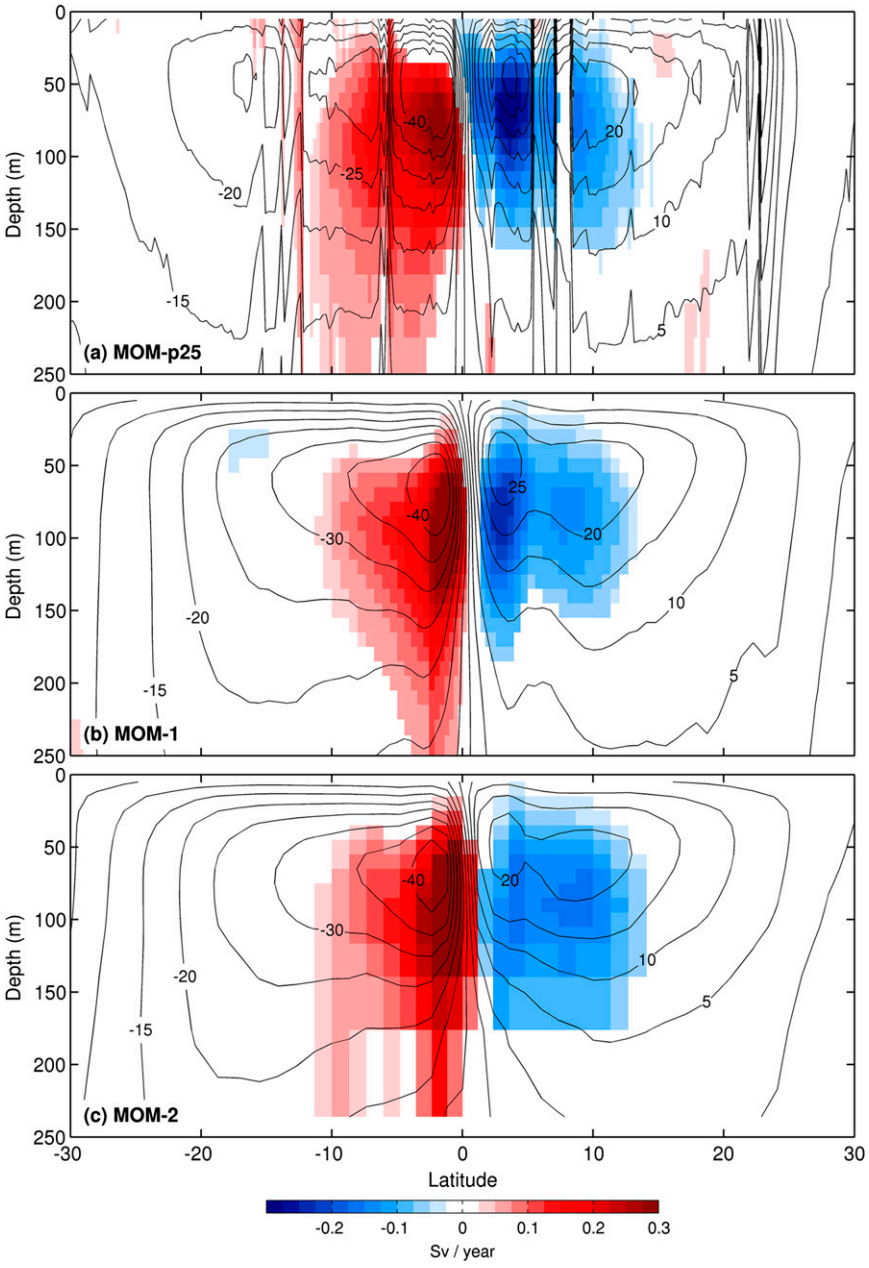

FIG. 1. Linear trend (Sv yr^{-1}) of the PMOC for (a) MOM-p25, (b) MOM-1, and (c) MOM-2. Contours represent the climatological streamfunction (Sv) defined as $\psi = \int v \, dz' \, dx$, where v is the meridional velocity, with clockwise circulation in the Northern Hemisphere and anticlockwise circulation in the Southern Hemisphere. Only trend values that are significant at the 95% level (evaluated using a two-tailed Student's t test) are displayed.

the later warming in the late twentieth century because of the weakening of the STC, and the trend toward negative values, which is coincident with the rebound of the STC circulation at the beginning of the twenty-first century. The low-frequency evolution in the HadISST record suggests that interdecadal variability is a robust feature of the equatorial Pacific Ocean during the twentieth century. Given the observed strong anticorrelation between STC and equatorial SST anomalies in the second half of the twentieth century supported by previous studies (MZ02; Nonaka et al. 2002; Cheng et al. 2007), it is tempting to extrapolate the relationship back to the full HadISST record as a low-frequency oscillation that spans over the entire twentieth century.

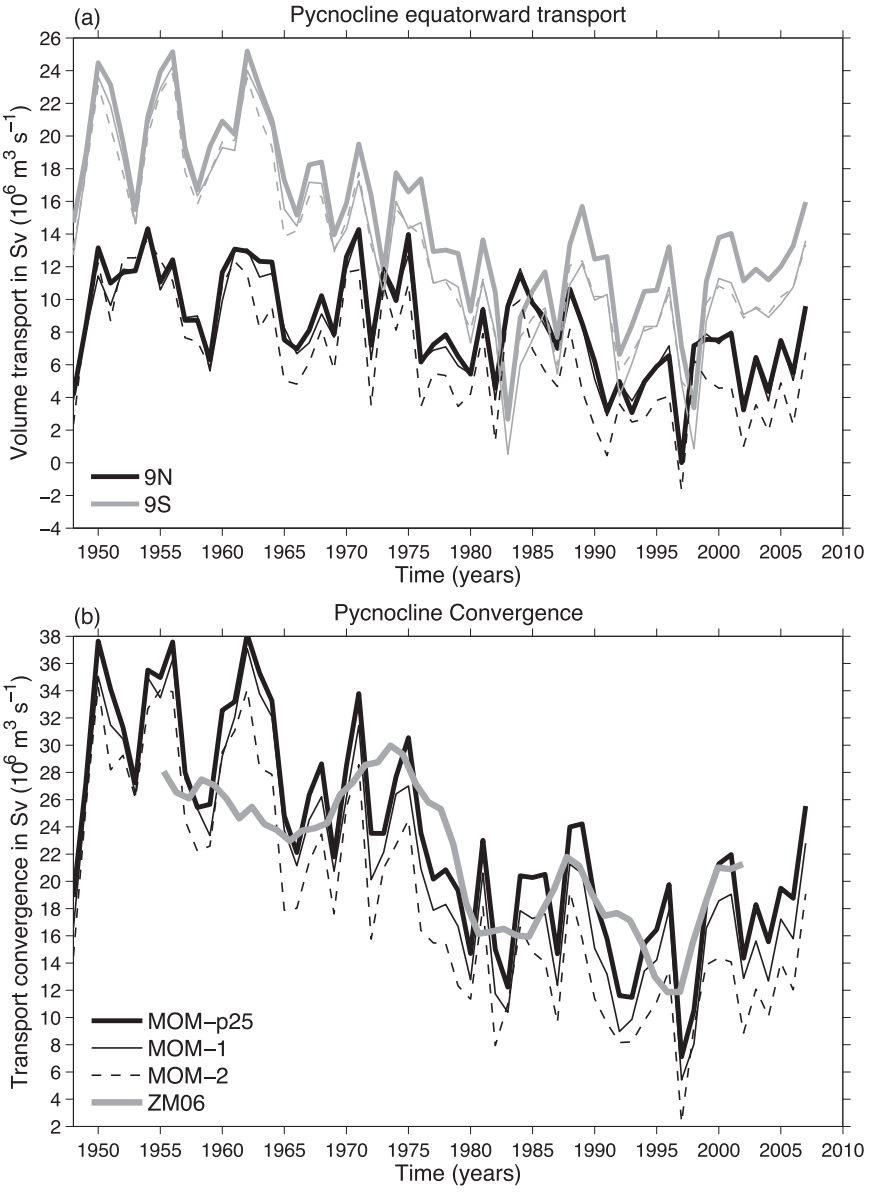

FIG. 2. (a) Annual-mean zonally integrated interior equatorward mass transports in the pycnocline across 9°N (black lines) and 9°S (gray lines) for the period 1948–2007. Transports are computed from the eastern boundary to 160°E in the SH and 145°E in the NH and between density classes σ_0 = 1022–1026 to capture the interior pathway of the pycnocline transport. Transports at 9°N have their sign reversed. Lines are for MOM-p25 (thick), MOM-1 (thin), and MOM-2 (dashed). (b) Annual-mean zonally integrated interior transport convergence, defined as the amount of transport moving equatorially across 9°N and 9°S. Lines are for MOM-p25 (thick), MOM-1 (thin), and MOM-2 (dashed). Also plotted are the observed interior STC transport convergence annual data from ZM06 (gray line).

Origin of equatorial anomalies

We have so far confirmed the sparse hydrographic data analysis presented in MZ02 and MZ04 and provided a reconstruction for the evolution of the shallow PMOC since 1948. We note that both MZ02 and MZ04 have invoked the possibility of tropical–subtropical interactions leading to the observed wind variability and the generation of ocean–atmosphere oscillations on decadal time scales (see also Kleeman et al. 1999). Molteni et al. (2011) recently suggested that subtropical wind stress and wind stress–curl anomalies related to extratropical internal

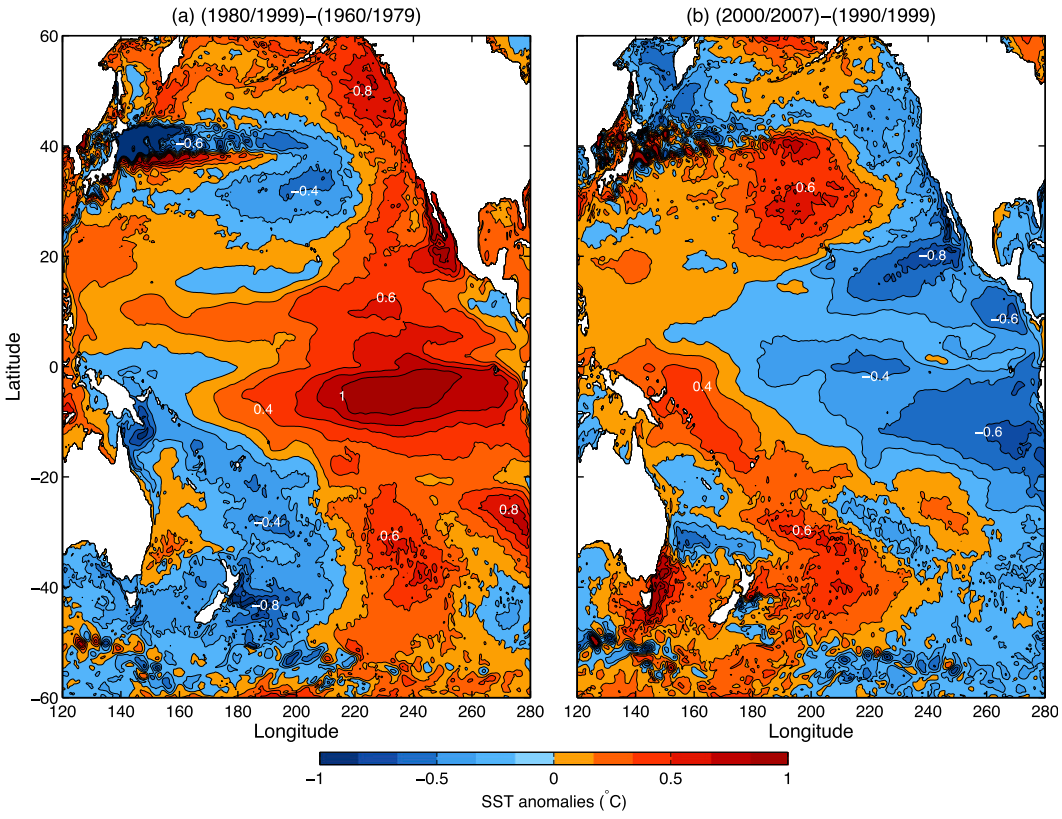

FIG. 3. Pacific SST (°C) anomalies for MOM-p25 computed as the difference between (a) the periods 1980–99 and 1960–79 and (b) the periods 2000–07 and 1990–99.

atmospheric variability of equatorial origin could be responsible for spinning up or down the Pacific Gyre circulation and, through Sverdrup balance, induce anomalies in interior pycnocline equatorward transport. This idea was further developed in Farneti et al. (2013), where the authors proposed a mechanism by which tropical SST interdecadal variability stems from the forcing of the subtropical Pacific through an atmospheric response to equatorial anomalies. The resulting Ekman pumping anomaly alters the STC, providing a negative feedback on the SST and generating a time-delayed response of the tropical oceans on a decadal time scale.

Figure 5a shows the difference in wind stress and its curl between the periods 1980–99 and 1960–79. Wind stress and wind stress–curl anomalous patterns within subtropical latitudes ($15° < \theta < 40°$) are in phase with climatological fields in both hemispheres. The anomalies will lead to a strengthening of the gyre and water subduction, equatorward geostrophic flow, and STC at the beginning of the twenty-first century. Following the mechanism proposed in Farneti et al. (2013), STC theories relating their strength to subtropical wind stress (McCreary and Lu 1994), and previous studies pointing to the role of subtropical winds in driving STC variability (Kleeman et al. 1999; Nonaka et al. 2002; Klinger et al. 2002; Solomon et al. 2003), we argue that subtropical wind anomalies presented in Fig. 5a are the main cause for the circulation rebound observed after 1998, which adjusts to the forcing on a decadal time scale. However, from the beginning of the twenty-first century onward, the observed subtropical patterns have reversed, as shown in Fig. 5b, where differences are presented for the periods 2000–07 and 1990–99. In light of the previous arguments, the pattern in Fig. 5b would be consistent with a weakening of the Pacific Subtropical Gyre and STC, so we expect a decreasing trend in the STC circulation and a warming of the equatorial Pacific in the following decade.

To test the origin of the low-frequency equatorial SST anomalies and STC transport, we performed two sensitivity experiments with the coarse-resolution model MOM-2. Both experiments start from the same initial conditions as in the MOM-2 simulation. First, we forced the ocean model with climatological winds. Not surprisingly, pycnocline transports at 9°N and 9°S were constant throughout the integration, and equatorial SSTs did not show any significant low-frequency variability (not shown). Then, similarly to Kleeman et al.

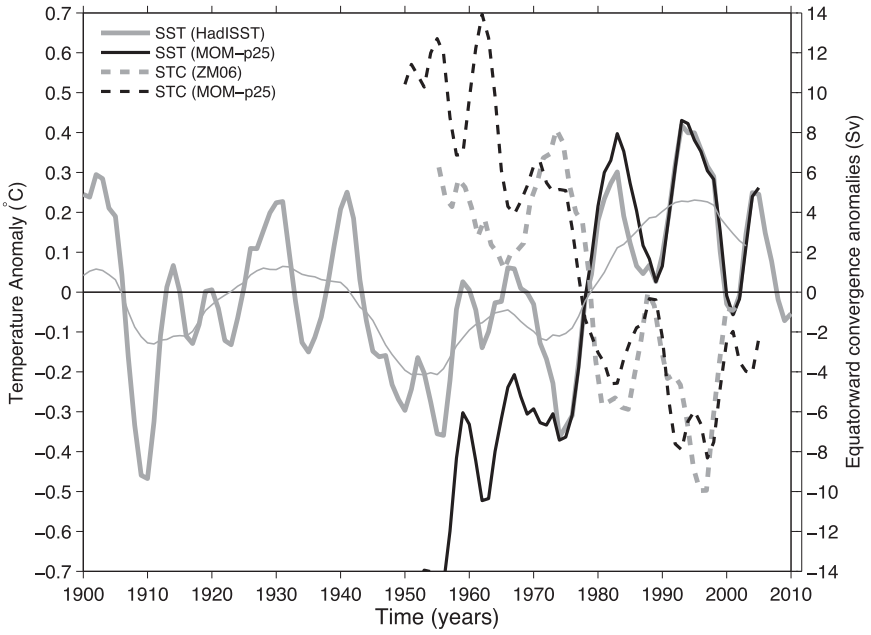

FIG. 4. SST (°C) anomalies in the equatorial Pacific Ocean and equatorward transport convergence (Sv). Gray continuous lines are for the HadISST reanalysis dataset smoothed twice with a 5-yr running mean (thick) and smoothed twice with a 10-yr running mean (thick); the black continuous line is SST from MOM-p25 smoothed twice with a 5-yr running mean. Transport convergence, i.e., equatorward transport across 9°N and 9°S, for the observed estimates of ZM06 (dashed gray) and for MOM-p25 smoothed twice with a 5-yr running mean (dashed black) are also plotted to highlight the anticorrelation with the SST. SST anomalies are averaged over the region 9°S–9°N and 180°–90°W and are relative to 1950–99 averages. During the first decade, both transport and SST anomalies from the model are less correlated with observations, probably because of biases in the initial conditions.

(1999) and Nonaka et al. (2002), we forced the ocean model with climatological winds within a 20°-wide cross-equatorial band ($10°S > \theta < 10°N$) and interannual winds elsewhere. The sensitivity experiment, called MOM-2-notrop, introduces sharp gradients near $\theta = 10°$, and not only the wind stress but also its curl will be affected. Nevertheless, it can be regarded as a first test on the origin of the low-frequency anomalies. Indeed, subtropical wind anomalies are known to drive significant changes in STC transport and hence equatorial upwelling and SST on decadal time scales, whereas tropical winds are mainly associated with interannual equatorial SST anomalies (Kleeman et al. 1999; Klinger et al. 2002; Solomon et al. 2003). As presented in Fig. 6, equatorward transport convergence anomalies are somewhat reduced compared to the full-forcing MOM-2 experiment, but the low-frequency component is still present, as well as most of the associated equatorial SST variability. The MOM-2-notrop experiment shows that the origin of the decadal signal lies outside the tropics.

The coarse-resolution model MOM-2 was characterized by the weakest transport variabilities, both in the weakening and rebound phase. The results of MOM-2-notrop can thus be considered a lower bound from our modeling suite. We also note that, during the first decade, SST anomalies from MOM-2-notrop are now more correlated with observations. The reduction in the discrepancies between model and observations can be attributed to a reduction in the biases originally generated by interannual equatorial winds and the initial oceanic state, confirming the importance of initialized oceanic conditions in hindcast simulations and climate change predictions (Guemas et al. 2013; Meehl and Teng 2014). It is also worth noting that, although transport anomalies are much reduced compared to the observational record, SST anomalies are relatively similar in magnitude to the HadISST dataset, pointing to an overly strong relationship between STC transport and equatorial SST in the model.

4. Discussion and conclusions

Global ocean–ice models, forced with atmospheric reanalysis datasets, have been used to study the evolution of the Pacific STCs and equatorial Pacific SST anomalies during the 1948–2007 period. Confirming and expanding recent observational results (MZ02; MZ04),

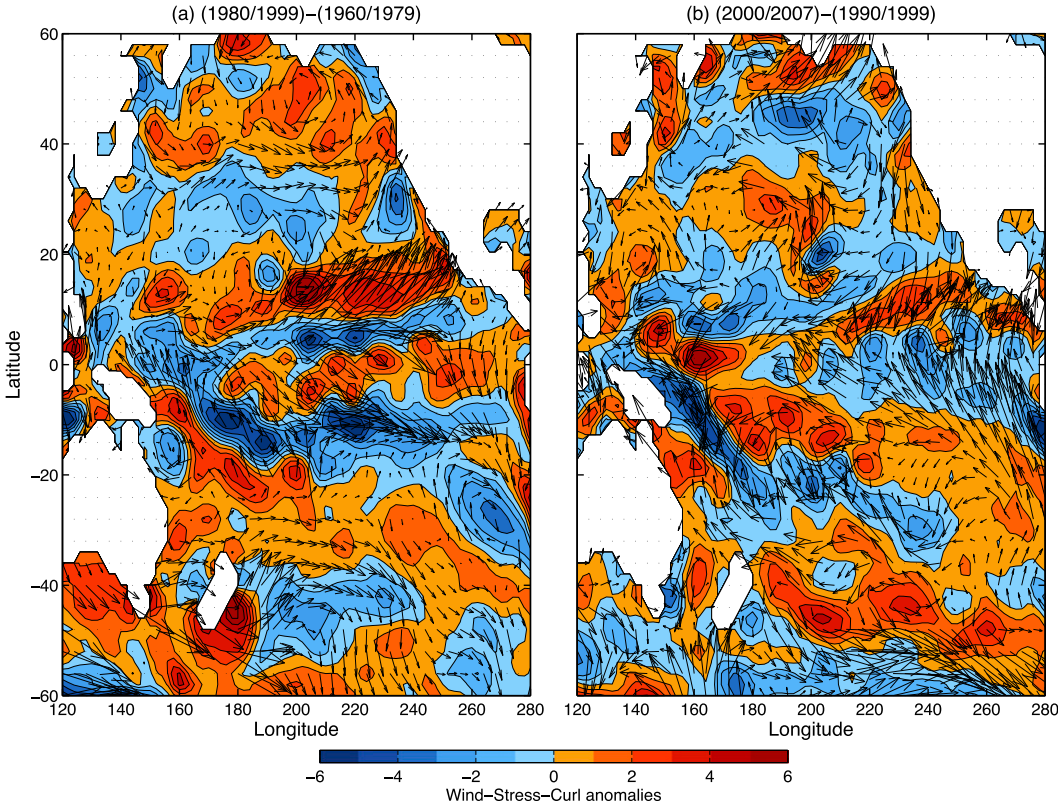

FIG. 5. Anomalies in wind stress (arrows; N m^{-2}) and its curl (shaded and scaled by 10^8) computed as the difference between (a) the periods 1980–99 and 1960–79 and (b) the periods 2000–07 and 1990–99.

we have shown that the STCs have experienced a decreasing trend until the late 1990s with a subsequent rebound in the first decade of the twenty-first century. The slowdown (rebound) in the STCs was associated with significant warming (cooling) of the equatorial Pacific.

The atmospheric subtropical variability was also analyzed and wind stress and wind stress–curl anomalies were identified as the cause that lead to a decadal timescale adjustment in the Pacific Subtropical Gyre, STC, and subsequent equatorial SST anomalies. Indeed, a sensitivity experiment where the ocean model was forced with interannual winds only poleward of 10° confirmed the primary role of off-equatorial winds in generating the oceanic low-frequency variability. Although SST anomalies are certainly generated by equatorial wind anomalies on interannual time scales (as evidenced by the large tropical anomalies in Fig. 5), the STCs are driven by wind stress at ~15° so that part of the low-frequency SST variability can only be explained through subtropical forcing.

This result is in agreement with ocean circulation theory that relates the strength of the STC to subtropical winds (McCreary and Lu 1994). In fact, intensified trades and negative subtropical wind stress–curl anomalies were followed by the circulation rebound at the end of the twentieth century. The low-frequency variability in STCs and SST anomalies shown in Figs. 2 and 4 are also consistent with the so-called mid-1970s and late 1990s climate shifts associated with the IPO (Trenberth and Hurrell 1994; Burgman et al. 2008). The rebound in STC transport and associated negative equatorial SST anomalies in the 2000s correspond with the recent hiatus in surface warming, of which equatorial Pacific SST anomalies are believed to be the main cause (Kosaka and Xie 2013; England et al. 2014). Moreover, straddling the year 2000, the atmospheric anomalies have reversed sign, so a weakening of the STCs and anomalous warming of the equatorial Pacific should be expected during and after the second decade of the twenty-first century. The natural quasi oscillation would then imply that the hiatus would cease and global warming would accelerate, as suggested in England et al. (2014).

Recently, Farneti et al. (2013) proposed a mechanism whereby extratropical atmospheric responses to tropical forcing have feedbacks on ocean dynamics, leading to a time-delayed response of the tropical oceans and giving rise to multidecadal coupled variability. The time

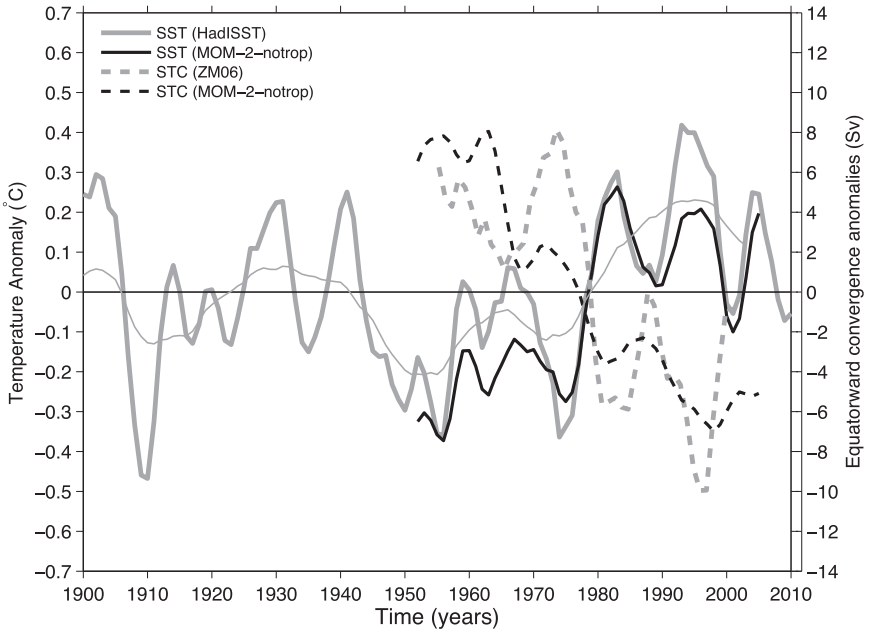

FIG. 6. As in Fig. 4, but for the experiment MOM-2-notrop, in which interannual winds are only present poleward of 10° and climatological winds are used equatorward of 10°. The transport and SST low-frequency variability, although reduced, is still present when the model is forced with interannual subtropical winds only. The coarse-resolution model MOM-2 showed the weakest weakening and rebound transport variabilities (see Fig. 2a). The results of MOM-2-notrop can thus be considered a lower bound from our modeling suite. During the first decade, both transport and SST anomalies from the model are now more correlated with observations, especially in the case of SSTs. This is probably due to a reduction in the biases generated by interannual equatorial winds and the uninitialized oceanic state.

scale is consistent with a baroclinic wave adjustment to wind stress anomalies of the Subtropical Gyre and STC, where the thermocline volume transport has been shown to equilibrate on decadal time scales (Klinger et al. 2002) and simulated particles take up to 15 years to reach the equatorial zone (Schott et al. 2004). Here, we have shown that the tropical–subtropical interaction is a viable mechanism for the Southern Hemisphere as well. The idealized model study of Farneti et al. (2013) presented a large asymmetry in the oceanic response. However, there is no dynamical constraint on the mechanism in the Southern Hemisphere, if not the opposite. Despite the IPO signal being somewhat stronger in the Northern Hemisphere with its PDO signature, the STC anomalies in the Southern Hemisphere are indeed stronger in both models and observations. In fact, interior circulation pathways from the subtropics to the equator are fundamentally different in the Northern and Southern Hemispheres of the Pacific Ocean. The high potential vorticity barrier in the Northern Hemisphere allows only a marginal meridional exchange within the central North Pacific, whereas the Southern Hemisphere presents a larger pathway from the southern subtropics to the equator (Lu and McCreary 1995; Johnson and McPhaden 1999; Huang and Wang 2001). The larger interior pathway in the Southern Hemisphere is well represented by the models, with much of the subducted anomalous water taking the interior route, which explains the larger transport anomalies of Fig. 2a.

Previous studies have already shown that decadal variations of tropical SSTs can be induced by changes in the subtropical winds (Kleeman et al. 1999; Klinger et al. 2002; Solomon et al. 2003), arguing that changes in equatorial SSTs are primarily related to changes in wind stress and subduction rates in the subtropics, as in Farneti et al. (2013) and this study. The observational records and state-of-the-art OGCM results thus corroborate and reinforce this hypothesis.

Recently, England et al. (2014) have attributed the circulation trends in the PMOC to intensified wind stress curl on either side of the equator, focusing on the role of tropical Pacific wind stress trends (6°N–6°S). We have argued here and in Farneti et al. (2013), with ocean-only and idealized simulations, that subtropical wind stress anomalies play a complementary role, if not bigger, in our modeling framework. Other natural factors, such as volcanic, solar, and aerosol variability, might modulate the magnitude and periodicity of the mechanism, and

Atlantic-Pacific teleconnections have also been shown to have an influence on equatorial Pacific SSTs (Kucharski et al. 2011). Disentangling the relative role of tropical and subtropical winds in generating low-frequency SST anomalies thus seems of paramount importance for the study of local and global climate variability and change. Progress could be achieved by performing idealized ''switched-on'' experiments by imposing artificial subtropical wind anomalies to an ocean model and studying the sensitivity of the equatorial ocean to the location, time dependence, and sign of the forcing anomaly.

Finally, contrary to coupled climate models, where the relationship between tropical Pacific SST and STCs is often absent (see discussion in Solomon and Zhang 2006), forced ocean–ice experiments provide a valuable tool for the simulation and understanding of the recent Pacific Ocean variability. A proper attribution of the observed relationship between subtropical wind stress, wind stress curl, and tropical ocean dynamics would require longer numerical integrations and the analysis of extended observations beyond the ones presented in MZ04, in order to examine a sufficient number of oscillations.

Acknowledgments. The authors thank the three anonymous reviewers for their insightful criticism, comments, and suggestions on the manuscript. SD thanks the Abdus Salam ICTP for providing facilities during his visits to the Centre as a junior associate. Thanks are also due to ISRO/MoES/DST for providing funds in the form of research projects. Thanks to Dr. Zhang and Dr. McPhaden for providing the observational data shown in Figs. 2 and 4. The CORE-II datasets are collaboratively supported by the National Center for Atmospheric research (NCAR) and the Geophysical Fluid Dynamics Laboratory under the umbrella of the CLIVAR Working Group on Ocean Model Development (WGOMD). All CORE datasets, support codes, and documentation are freely available at: http://data1.gfdl.noaa.gov/nomads/forms/core/COREv2.html.

REFERENCES

Burgman, R. J., A. C. Clement, C. M. Mitas, J. Chen, and K. Esslinger, 2008: Evidence for atmospheric variability over the Pacific on decadal timescales. *Geophys. Res. Lett.,* **35,** L01704, doi:10.1029/2007GL031830.

Cheng, W., M. J. McPhaden, D. Zhang, and E. J. Metzger, 2007: Recent changes in the Pacific subtropical cells inferred from an eddy-resolving ocean circulation model. *J. Phys. Oceanogr.,* **37,** 1340–1356, doi:10.1175/JPO3051.1.

Collins, M., and Coauthors, 2010: The impact of global warming on the tropical Pacific Ocean and El Niño. *Nat. Geosci.,* **3,** 391–397, doi:10.1038/ngeo868.

Danabasoglu, G., and Coauthors, 2014: North Atlantic simulations in Coordinated Ocean–Ice Reference Experiments phase II (CORE-II). Part I: Mean states. *Ocean Modell.,* **73,** 76–107, doi:10.1016/j.ocemod.2013.10.005.

Delworth, T. L., and Coauthors, 2012: Simulated climate and climate change in the GFDL CM2.5 high-resolution coupled climate model. *J. Climate,* **25,** 2755–2781, doi:10.1175/JCLI-D-11-00316.1.

Dunne, J. P., and Coauthors, 2012: GFDL's ESM2 global coupled climate–carbon Earth System Models. Part I: Physical formulation and baseline simulation characteristics. *J. Climate,* **25,** 6646–6665, doi:10.1175/JCLI-D-11-00560.1.

England, M. H., and Coauthors, 2014: Recent intensification of wind-driven circulation in the Pacific and the ongoing warming hiatus. *Nat. Climate Change,* **4,** 222–227, doi:10.1038/nclimate2106.

Farneti, R., F. Molteni, and F. Kucharski, 2013: Pacific interdecadal variability driven by tropical–extratropical interactions. *Climate Dyn.,* **42,** 3337–3355, doi:10.1007/s00382-013-1906-6.

Fedorov, A. V., and S. G. H. Philander, 2001: A stability analysis of tropical ocean–atmosphere interactions: Bridging measurements and theory for El Niño. *J. Climate,* **14,** 3086–3101, doi:10.1175/1520-0442(2001)014<3086:ASAOTO>2.0.CO;2.

Ferrari, R., S. M. Griffies, A. J. G. Nurser, and G. K. Vallis, 2010: A boundary-value problem for the parameterized mesoscale eddy transport. *Ocean Modell.,* **32,** 143–156, doi:10.1016/j.ocemod.2010.01.004.

Fox-Kemper, B., and Coauthors, 2011: Parameterization of mixed layer eddies. III: Implementation and impact in global ocean climate simulations. *Ocean Modell.,* **39,** 61–78, doi:10.1016/j.ocemod.2010.09.002.

Fyfe, J. C., N. P. Gillett, and F. W. Zwiers, 2013: Overestimated global warming over the past 20 years. *Nat. Climate Change,* **3,** 767–769, doi:10.1038/nclimate1972.

Griffies, S. M., and Coauthors, 2005: Formulation of an ocean model for global climate simulations. *Ocean Sci.,* **1,** 45–79, doi:10.5194/os-1-45-2005.

——, and Coauthors, 2009: Coordinated Ocean–Ice Reference Experiments (COREs). *Ocean Modell.,* **26,** 1–46, doi:10.1016/j.ocemod.2008.08.007.

Guemas, V., F. J. Doblas-Reyes, I. Andreu-Burillo, and M. Asif, 2013: Retrospective prediction of the global warming slowdown in the past decade. *Nat. Climate Change,* **3,** 649–653, doi:10.1038/nclimate1863.

Huang, R. X., and Q. Wang, 2001: Interior communication from the subtropical to the tropical oceans. *J. Phys. Oceanogr.,* **31,** 3538–3550, doi:10.1175/1520-0485(2001)031<3538:ICFTST>2.0.CO;2.

Johnson, G. C., and M. J. McPhaden, 1999: Interior pycnocline flow from the subtropical to the equatorial Pacific Ocean. *J. Phys. Oceanogr.,* **29,** 3073–3089, doi:10.1175/1520-0485(1999)029<3073:IPFFTS>2.0.CO;2.

Kleeman, R., J. P. McCreary, and B. A. Klinger, 1999: A mechanism for generating ENSO decadal variability. *Geophys. Res. Lett.,* **26,** 1743–1746, doi:10.1029/1999GL900352.

Klinger, B. A., J. P. McCreary, and R. Kleeman, 2002: The relationship between oscillating subtropical wind stress and equatorial temperature. *J. Phys. Oceanogr.,* **32,** 1507–1521, doi:10.1175/1520-0485(2002)032<1507:TRBOSW>2.0.CO;2.

Kosaka, Y., and S.-P. Xie, 2013: Recent global-warming hiatus tied to equatorial Pacific surface cooling. *Nature,* **501,** 403–407, doi:10.1038/nature12534.

Kucharski, F., I.-S. Kang, R. Farneti, and L. Feudale, 2011: Tropical Pacific response to 20th century Atlantic warming. *Geophys. Res. Lett.,* **38,** L03702, doi:10.1029/2010GL046248.

Large, W. G., and S. G. Yeager, 2009: The global climatology of an interannually varying air–sea flux data set. *Climate Dyn.,* **33,** 341–364, doi:10.1007/s00382-008-0441-3.

Liu, Z., 1994: A simple model of the mass exchange between the subtropical and tropical ocean. *J. Phys. Oceanogr.,* **24,** 1153–1165, doi:10.1175/1520-0485(1994)024<1153:ASMOTM>2.0.CO;2.

Lu, P., and J. P. McCreary, 1995: Influence of the ITCZ on the flow of thermocline water from the subtropical to the equatorial Pacific Ocean. *J. Phys. Oceanogr.,* **25,** 3076–3088, doi:10.1175/1520-0485(1995)025<3076:IOTIOT>2.0.CO;2.

——, ——, and B. A. Klinger, 1998: Meridional circulation cells and the source waters of the Pacific Equatorial Undercurrent. *J. Phys. Oceanogr.,* **28,** 62–84, doi:10.1175/1520-0485(1998)028<0062:MCCATS>2.0.CO;2.

Mantua, N. J., S. R. Hare, Y. Zhang, J. M. Wallace, and R. Francis, 1997: A Pacific interdecadal climate oscillation with impacts on salmon production. *Bull. Amer. Meteor. Soc.,* **78,** 1069–1079, doi:10.1175/1520-0477(1997)078<1069:APICOW>2.0.CO;2.

McCreary, J. P., and P. Lu, 1994: Interaction between the subtropical and equatorial ocean circulations: The subtropical cell. *J. Phys. Oceanogr.,* **24,** 466–497.

McPhaden, M. J., and D. Zhang, 2002: Slowdown of the meridional overturning circulation in the upper Pacific Ocean. *Nature,* **415,** 603–608, doi:10.1038/415603a.

——, and ——, 2004: Pacific Ocean circulation rebounds. *Geophys. Res. Lett.,* **31,** L18301, doi:10.1029/2004GL020727.

Meehl, G. A., and H. Teng, 2014: CMIP5 multi-model hindcasts for the mid-1970s shift and early 2000s hiatus and predictions for 2016–2035. *Geophys. Res. Lett.,* **41,** 1711–1716, doi:10.1002/2014GL059256.

——, A. Hu, J. M. Arblaster, J. Fasullo, and K. E. Trenberth, 2013: Externally forced and internally generated decadal climate variability associated with the interdecadal Pacific oscillation. *J. Climate,* **26,** 7298–7310, doi:10.1175/JCLI-D-12-00548.1.

Molteni, F., M. P. King, F. Kucharski, and D. M. Straus, 2011: Planetary-scale variability in the northern winter and the impact of land–sea thermal contrast. *Climate Dyn.,* **37,** 151–170, doi:10.1007/s00382-010-0906-z.

Nonaka, M., S.-P. Xie, and J. P. McCreary, 2002: Decadal variations in the subtropical cells and equatorial Pacific SST. *Geophys. Res. Lett.,* **29,** 1116, doi:10.1029/2001GL013717.

Rayner, N. A., D. E. Parker, E. B. Horton, C. K. Folland, L. V. Alexander, D. P. Rowell, E. C. Kent, and A. Kaplan, 2003: Global analyses of sea surface temperature, sea ice, and night marine air temperature since the late nineteenth century. *J. Geophys. Res.,* **108,** 4407, doi:10.1029/2002JD002670.

Schott, F. A., J. P. McCreary, and G. C. Johnson, 2004: Shallow overturning circulations of the tropical–subtropical oceans. *Earth's Climate: The Ocean–Atmosphere Interaction, Geophys. Monogr.,* Vol. 147, Amer. Geophys. Union, 261–304.

——, W. Wang, and D. Stammer, 2007: Variability of Pacific subtropical cells in the 50-year ECCO assimilation. *Geophys. Res. Lett.,* **34,** L05604, doi:10.1029/2006GL028478.

Solomon, A., 2010: Interannual ENSO variability forced through coupled atmosphere–ocean feedback loops. *Geophys. Res. Lett.,* **37,** L02706, doi:10.1029/2009GL041622.

——, and D. Zhang, 2006: Pacific subtropical cell variability in coupled climate model simulations of the late 19th–20th century. *Ocean Modell.,* **15,** 236–249, doi:10.1016/j.ocemod.2006.03.007.

——, J. P. McCreary, R. Kleeman, and B. A. Klinger, 2003: Interannual and decadal variability in an intermediate coupled model of the Pacific region. *J. Climate,* **16,** 383–405, doi:10.1175/1520-0442(2003)016<0383:IADVIA>2.0.CO;2.

Trenberth, K. E., and J. W. Hurrell, 1994: Decadal atmosphere–ocean variations in the Pacific. *Climate Dyn.,* **9,** 303–319, doi:10.1007/BF00204745.

Zhang, D., and M. J. McPhaden, 2006: Decadal variability of the shallow Pacific meridional overturning circulation: Relation to tropical sea surface temperatures in observations and climate change models. *Ocean Modell.,* **15,** 250–273, doi:10.1016/j.ocemod.2005.12.005.